Journal of Construction Engineering, Management & Innovation
2018 Volume 1 Issue 1 Pages 1-17
https://doi.org/10.31462/jcemi.2018.01001017

www.goldenlightpublish.com

RESEARCH ARTICLE

Assessment of the thermal performance of holistic flat roof systems of industrial buildings

A.P. van Lith, A.G. Entrop and J.I.M. Halman*

University of Twente, Department of Construction Management and Engineering, Enschede, The Netherlands

Abstract

The thermal performance of conventional flat roof systems is in practice normally assessed by the heat transfer caused by conduction. The effects of radiation and convection are in such cases ignored as being insignificant. Holistic flat roof systems are designed to better utilize the impact of radiation and convection on improving the indoor climate. However, to determine the influence of radiation and convection, an integrated assessment should be used. In this article, the effect of applying five different holistic flat roof systems is compared with a conventional roof system of an existing storage hall. With EnergyPlus the internal air temperature in the storage hall was simulated for a complete year using weather data of the moderate Dutch climate. The most efficient systems prove to be the systems that decrease the heat gain by solar radiation. These systems can decrease the number of overheating hours by up to 95%. Increasing the thermal resistance value of a roof could lead to adverse results. The study shows an integrated approach that could be implemented in policies and regulations for the thermal assessment of holistic flat roof systems.

Keywords

Building simulation; Indoor climate; Heat transfer; Conduction; Convection; Radiation

Received: 14 March 2018; Accepted: 23 March 2018
ISSN: 2630-5771 (online)

1. Introduction

A flat roof is an often used design for industrial buildings. Flat roofs in different climates are usually covered with a dark coloured roofing material [1–4]. The temperature of this dark coloured roofing material can, on sunny summer days, primarily due to solar radiation, rise to 90 °C [5]. Akbari et al. [6] found that the difference between the surface temperature and the ambient air temperature can be as much as 50 °C with dark roofs. The term flat roof system is here used for a horizontal roof made up of multiple layers of different materials that together determine and influence the thermal performance of the building. Decreasing the roof temperature is nowadays widely accepted as a significant way of improving the summer thermal comfort in buildings [4, 7]. In winter, in moderate climates, the heat flow through flat roofs is mainly upwards (heat leaving the building) and a layer of insulation may be added to the building shell to decrease this conductive heat flow.

In general, to determine conductive losses, the thermal resistances of the individual layers of a roof are summed to find a static R-value (expressed in m^2K/W) or U-value (expressed in W/m^2K) for the roof structure. Adding insulation material to the

* Corresponding author
Email: j.i.m.halman@utwente.nl

roof increases the R-value and decreases conductive heat losses. The roof insulation acts as a barrier to heat flow in both directions. In summer, it will first act as a barrier to limit the heat contained in the warm outside air transferring to the cooler internal space through conduction. However, at some point, a temperature equilibrium will be reached and the heat flow will cease and then reverse, and the insulation will hinder natural cooling by conduction.

An assessment that focuses on conduction as the only heat transfer method overlooks a number of opportunities to improve the indoor climate. Assessments of flat roof systems to comply with building regulations and to operate as input for energy performance indicators [8], often only include conduction as the heat transfer method. The effects of radiation and convection are, often wrongly, ignored as insignificant. By not including radiation and convection in the design assessment, the space for innovative solutions is unnecessarily reduced. Bahadori [as cited in 9] explains, as a first example, that curved roofs are liable to incur higher convective heat losses than flat roofs under similar levels of solar irradiance. Suehrcke et al. [4] also noted that heat transfer types, other than conduction, were ignored in energy performance regulations and, for a second example, reflects on the possible positive and negative effects of the roof colour. In general, ignoring convection and radiation probably underestimates the potential added-value of innovative and advanced flat roof systems.

This study focuses on the contributions that a holistic flat roof system can make to improve the indoor climate of an existing flat-roofed building. The term holistic is used to refer to flat roof systems that are designed taking multiple heat transfer methods into account [10]. For clarity, although the term holistic could be interpreted broader than the heat transfer mechanisms (e.g. daylight usage and acoustic properties), the term holistic in this article refers only to heat transfer methods.

The objective of this study is to offer guidance on improving the indoor climate in buildings by providing a comparative assessment of a range of holistic flat roof systems. Consequently, a calculation method is used that can be applied to different holistic flat roof systems and that takes conduction, convection, and radiation of heat into account.

2. Holistic flat roof systems

There are various types of holistic flat roof systems. Five holistic flat roof systems have been selected that potentially improve the indoor climate by utilizing other heat transfer methods. Both cool roofs and green roofs could decrease the heat gain from solar radiation [5, 11]. Further, a double-skin roof (DSR) is an option for increasing convection losses by adding a layer that is separated from the conventional roof with a cavity. Finally, the Roofclix system is a relatively new system that has been designed with attention given to all three heat transfer methods.

2.1. Cool roofs

Increasing the albedo (α) of the top layer of a roof increases the reflection of sunlight and decreases the effect of solar radiation on the inside temperature. If a surface, exposed to solar radiation, has a high albedo, the resulting temperature increase will be lower than for a surface with a low albedo. The Infrared emittance (σ) is used to specify the amount of radiation that is emitted and absorbed compared to a black body, which is a perfect emitter and absorber of radiation. Both the albedo and the infrared emittance are measured on a 0 to 1 scale. The albedo of asphalt roofing is typically around 0.1 [12], while the albedo of the external wall of the case object is estimated at 0.37 [13]. The infrared emittance of non-metallic surfaces is typically about 0.9 [4].

The literature often uses the terms white roof, high albedo roof, and cool roof interchangeably. The concept of a cool roof is described by Dabaieh et al. [14] as “a passive solution and a building typology that assists in reducing the cooling loads and energy demands on a building’s envelope”. According to ASHRAE standards, a cool roof has an albedo ≥ 0.70 and an emittance ≥ 0.75 [15]. In

this paper, the term cool roof will be used since not all cool roofs are white [16].

A cool roof can be created by adding a layer with a high albedo to an existing roof [e.g. 12,17] or by replacing the existing top layer with a highly reflective material. A relatively cheap method of increasing the albedo is simply to paint the roof. Kolokotroni et al. [12] found that a cool roof could decrease the internal air temperature by an average of 2.5 °C for an office in London. Romeo and Zinzi [18] similarly found an average reduction of 2.3 °C using a cool roof in the operative temperature during the cooling season for a school in Italy.

A cool roof gains heat by absorbing shortwave solar radiation and longwave diffuse radiation and loses heat by emitting longwave radiation. Natural convection takes place on the surface and conduction through the roof. The energy balance for a cool roof system is given by Eq. (1).

$$F_c = \alpha_c I_S - \sigma\varepsilon_c\left(T_c^4 - T_{sky}^4\right) - \frac{T_c - T_i}{R_c + R_r} + H_c \qquad (1)$$

2.2. Green roofs

A green roof is created by planting vegetation on the roof, and these have been assessed in several studies [e.g. 1, 19]. Coma et al. [19] state that green roofs are "interesting construction systems because they provide both aesthetic and environmental benefits". A major contribution of green roofs in terms of thermal comfort is the protection they provide against solar radiation [20].

Ismail et al. [11] found indoor air temperature differences between green and bare black roofs in Malaysia that ranged from 0.2 °C to 1.7 °C. Niachou et al. [20] found a green roof improved summer indoor comfort conditions by 2.0 °C in Greece. Gagliano et al. [21] found that a green roof can decrease the operative temperature by more than 3.0 °C compared with an uninsulated roof in Italy.

When assessing green roofs, a distinction is made between the energy balance for the foliage and for the substrate since the foliage layer is semi-transparent. Both the foliage and the substrate experience convection and solar radiation. There is a strong relationship between these two energy balances. The substrate layer is an opaque layer and therefore the heat flux between the substrate layer and the conventional roof below it is purely conductive. The heat balances for the foliage and the substrate layers are given in Eqs. (2) and (3) [22,23]. The interested reader is referred to Sailor [23].

$$F_f = \alpha_f\left(I_S\alpha_f + \varepsilon_f I_{ir} - \varepsilon_f\sigma T_f^4\right) + \frac{\sigma_f\varepsilon_g\varepsilon_f\sigma}{\varepsilon_g + \varepsilon_f - \varepsilon_g\varepsilon_f}\left(T_g^4 - T_f^4\right) + H_f + L_f \qquad (2)$$

$$F_g = \left(1-\alpha_f\right)\left(I_S\alpha_g + \varepsilon_g I_{ir} - \varepsilon_g T_g^4\right) - \frac{\sigma_f\varepsilon_g\varepsilon_f\sigma}{\varepsilon_g + \varepsilon_f - \varepsilon_g\varepsilon_f}\left(T_g^4 - T_f^4\right) + H_g + L_g - \frac{T_g - T_i}{R_g + R_r} \qquad (3)$$

2.3. Roofs covered with PV panels

PV panels on a roof not only transform solar energy into electrical energy that can be used in the building, they also provide shading [24,25]. While there has been considerable research on the feasibility of placing PV panels on roofs, this has mainly focused on the financial and environmental benefits of the electric energy provided by the solar panels.

Wang [26] states that separating PV panels from the roof by incorporating a cavity decreases the cooling load and increases the efficiency of the PV panels. For maximum shading on a flat roof, the PV panels should be parallel to the roof, in other words, placed horizontally. If so placed, the efficiency of the panels will be sub-optimum, but a high output can still be achieved. Kapsalis et al. [27] measured, on a typical summer day in Greece, a roof surface temperature variability of almost 40 °C for an exposed roof, while the temperature variability under a roof covered in PV panels was less than 20 °C. Further, the minimum outside surface temperature of the exposed roof was lower than that of the shaded roof.

The heat transfer mechanisms of a roof covered with PV panels parallel to the roof can be expressed

by two energy balances (Eqs. (4) and (5)). The gap between the roof and the panels allows convection and radiation. The energy balance for the PV panels includes two sensible heat fluxes as convection can take place on both sides of the panels.

$$F_{PV} = \alpha_{PV} I_S - \sigma\varepsilon_t \left(T_t^4 - T_{sky}^4\right) + \frac{\varepsilon_b \varepsilon_t \sigma}{\varepsilon_b + \varepsilon_t - \varepsilon_b \varepsilon_t}\left(T_t^4 - T_b^4\right) + \frac{T_t - T_b}{R_{PV}} + H_t + H_b \quad (4)$$

$$F_r = \frac{\varepsilon_b \varepsilon_r \sigma}{\varepsilon_b + \varepsilon_r - \varepsilon_b \varepsilon_r}\left(T_r^4 - T_b^4\right) - \frac{T_r - T_i}{R_r} + H_r \quad (5)$$

2.4. Double roof

Creating a non-ventilated cavity (i.e. close-ended) by placing a double roof above an existing one provides a barrier to heat entering or escaping from the room. Another option is a ventilated open-ended cavity, where the cavity and the second layer can decrease the cooling load on a building. The 'second' roof provides shelter against solar radiation [28,29].

Zingre et al. [28] note a maximum reduction in indoor air temperature of 2.4 °C on a sunny day and 1.1 °C on a cloudy day for an open-ended double roof in the tropical climate of Singapore. In comparison, Gagliano et al. [21] found that adding a 40 mm layer of insulation to an uninsulated roof decreased the operative temperature by a not-dissimilar 2.0 °C. Considering a situation in a moderate climate and comparable to the use of PV panels, Eq. (6) provides the heat balance for a close-ended double roof system.

$$F_{dr} = \alpha_{dr} I_S - \sigma\varepsilon_{dr}\left(T_{dr}^4 - T_{sky}^4\right) - \frac{T_{dr} - T_i}{R_{dr} + R_{cav} + R_r} + H_{dr} \quad (6)$$

2.5. Roofclix system

The Roofclix system is a relatively new and largely unknown holistic flat roof system. The system is shown in Fig. 1. It consists of highly reflective 400mm x 400mm polyvinyl chloride (PVC) panels that are 40 mm deep and filled with polyurethane (PUR) with a high thermal resistance. The panels are fixed above the existing roof using coupling pieces with a diameter of 260 mm and a height of 65 mm. These coupling pieces raise the Roofclix panels creating a cavity of 25 mm between the roof and the panels. The gaps between the Roofclix panels have an area of 3,960 mm^2 per square meter or 4.0% of the total area. As such, the cavity under the Roofclix system is a well-ventilated air layer in terms of ISO 6946. The Roofclix panels have, according to the supplier of the system, an albedo value of 0.85 and weigh 8 kg per m^2 [30]. Neglecting the small impact of the PUR, the specific heat capacity of the panels is 840 J/kgK [13]. The energy balance for the roof with the Roofclix system is presented in Eq. (7) where, based on ISO 6946, R_{cav}=0.06 m^{2}K/W and R_{rx}= 0.

$$F_{rx} = \alpha_{rx} I_S - \sigma\varepsilon_{rx}\left(T_{rx}^4 - T_{sky}^4\right) - \frac{T_{rx} - T_i}{R_{rx} + R_{cav} + R_r} + H_{rx} \quad (7)$$

3. Method

This section presents how holistic flat roof systems will be studied by modeling their effects on indoor temperature when applied to a particular building, referred to as our case object. The research design is in line with the approaches of Boyano et al. [31] and Dabaieh et al. [14] in that the measures are not physically placed on the case object but implemented in a simulation.

Several energy simulation programs (ANSYS, TRNSYS) are available and were considered. EnergyPlus will be used in this research. Positive experiences of this open-source software are reported in comparable studies [14,31].

Fig. 1. The Roofclix system

The research process consists of the following steps:

1. Assessing of the relevant heat transfer methods when applying a particular roof design;
2. Deriving the energy balance for the adopted roof design;
3. Implementing the roof design in Energyplus;
4. Checking the validity of assumptions;
5. Running EnergyPlus for multiple scenarios;
6. Analyzing the effect of the roof design on the thermal comfort.

3.1. Climate data

A local IWEC weather data file was obtained for Groningen (Eelde) Airport (latitude: 53° 7' 11" N, longitude 6° 34' 46" E) which has comparable weather conditions. The Netherlands is, in terms of the ASHRAE standard, located in the Cool-Humid climate zone 5A [15]. The meteorological institute in the Netherlands (KNMI) indicates that the monthly mean temperature varies between 3.1 °C in January and 17.9 °C in July [32]. On average the annual precipitation is 887 mm [33] and the long-term mean solar radiation intensity is 10.1 $MJm^2(day)^{-1}$ [34].

To be able to calibrate the EnergyPlus model for the case object's current roof system, three temperature sensors (RTD Pt1000) were installed to measure indoor temperatures. Over a period of four weeks, from 25 September 2015 to 23 October 2015, these sensors were connected to a data logger (ATAL ATV-05A). This time period was chosen by the owner of the facility, who granted us permission to measure. Considering that the average outdoor temperature we measured during this time period was 9.6 ºC and is close to the national annual average of 9.5 ºC, we believe that this relative short period can be considered as representative. The temperature was measured at three heights close to the center of the storage facility. Sensor 1 was placed 0.3 m below the roof. Sensor 2 was placed at a height of 3.0 m above the floor to measure air temperature development within the hall. Sensor 3 was placed 1.0 m above the floor to measure the air temperature experienced by people in the storage hall. Fig. 2 shows a schematic view of the position of the sensors.

3.2. Building model

In previous studies, the implementation of holistic flat roof systems has been studied for various building types (e.g. dwellings [35], schools [18], industrial buildings [36] and offices [37]). We focus on industrial buildings since these are known for their relatively large flat roofs resulting in high 'roof-to-wall' ratios. As such, their roofs are expected to have a considerable influence on the indoor climate. Our case object is an existing storage hall of an industrial company as shown in Fig. 3. The building is located in the north-eastern part of the Netherlands. The building specification reflects typical designs from around 25 years ago, and the storage hall is connected on its north side to other parts of the factory. The other three sides are external walls and not shaded by surrounding objects. As a storage facility, there is only limited activity within it. Personnel works in the storage hall at irregular moments. The duration of the working tasks in the storage hall range from a few minutes to several hours. Production continues 24 hours per day and seven days per week.

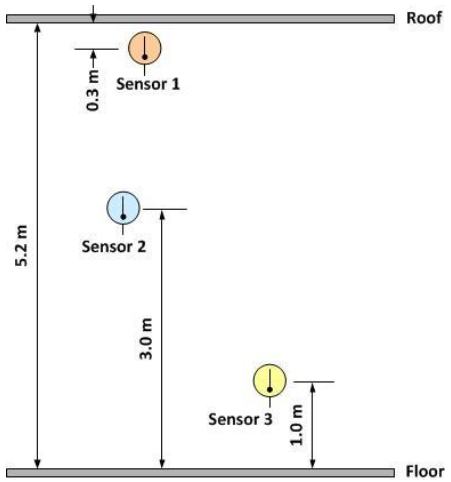

Fig. 2. Position of the temperature sensors

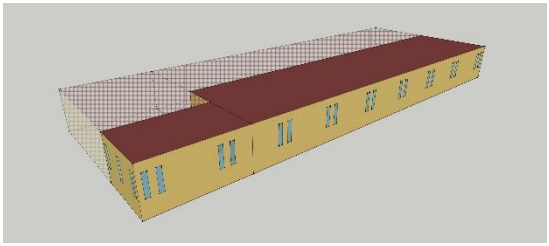

Fig. 3. The case object in SketchUp (The transparent spaces are not part of the case object, but are simulated as adjacent buildings to include their thermal influence on the case object)

The hall has an internal floor area of 686 m^2 and the internal height is 5.2 m. In terms of temperature control, the storage hall has a heating but no cooling system. The thermal resistance of the building envelope, presented in Table 1, was calculated in line with ISO 6946 [38] based on the original building plans. The typical structure of such a roof for an industrial building is shown in Fig. 4. The current insulation material is placed above the structural layer, making the current roof a so-called 'warm roof', and its thermal resistance is calculated at 3.5 m^2K/W.

Table 1. Thermal characteristics of the building envelope of the case object

Construction element	Materials	d (m)	λ (W/mK)	ρ (kg/m^3)	Specific heat capacity (J/kg K)
External wall	Sand-lime brick	0.100	0.860	1,850	840
	Cavity	0.030	-	1.20	1,010
	Rockwool insulation	0.040	0.038	25	840
	Brickwork	0.100	0.770	1,700	835
Roof	Cellular concrete	0.140	0.160	727	840
	PUR insulation material	0.060	0.025	30	1,470
	Asphalt	0.030	0.700	2,100	840
Floor	Monolith concrete layer	0.150	1.930	2,450	840

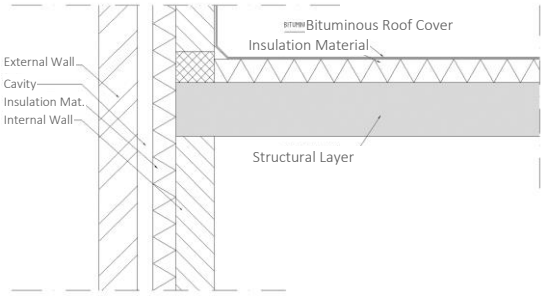

Fig. 4. Typical construction of a bituminous roof of an industrial building

The internal heat gains in the storage hall are linked to the lighting system with a power density of 3.9 W/m^2. The storage hall has twenty-one fixed exterior windows (2.50 m x 0.50 m) consisting of double glazing in an aluminum frame with a heat transfer coefficient around 3.1 W/m^2K and three interior high-speed roll-up doors (3.00 m x 2.00 m) with a heat transfer coefficient estimated at 2.4 W/m^2K.

3.3. Scenarios

The thermal resistance of the roof has a major effect on the thermal performance of a building. Therefore, two scenarios are simulated to investigate the influence of the thermal resistance of the existing roof on the effect of a holistic flat roof system. First, we model a high thermal resistance scenario, with an R-value of 3.5 m^2K/W. This is in line with the calculated value for the storage hall we are simulating. Second, we investigate a low thermal resistance construction that can be seen as similar to the first scenario but without the layer of insulation material in the roof, resulting in an R-value is 1.1 m^2K/W. Combining these two scenarios with the six roof designs outlined earlier results in twelve situations as shown in Fig. 5.

3.4. Holistic flat roof systems

The building has been modeled in EnergyPlus including heating, ventilation and lighting influences. The heat gains from the adjacent production hall are simulated as a thermal load on

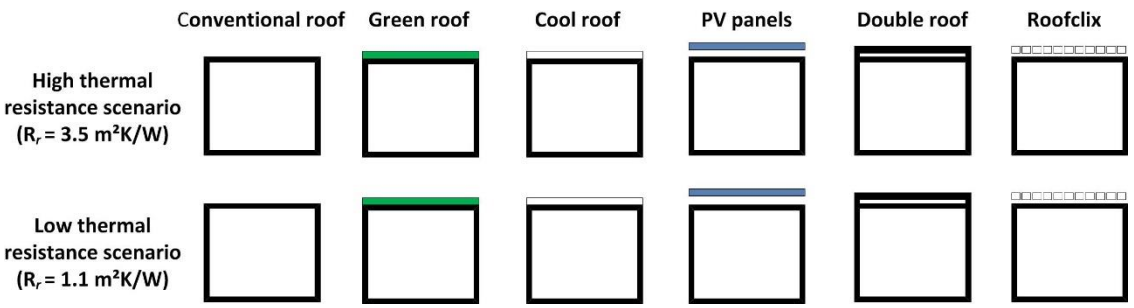

Fig. 5. The scenarios and holistic flat roof systems used in the simulations

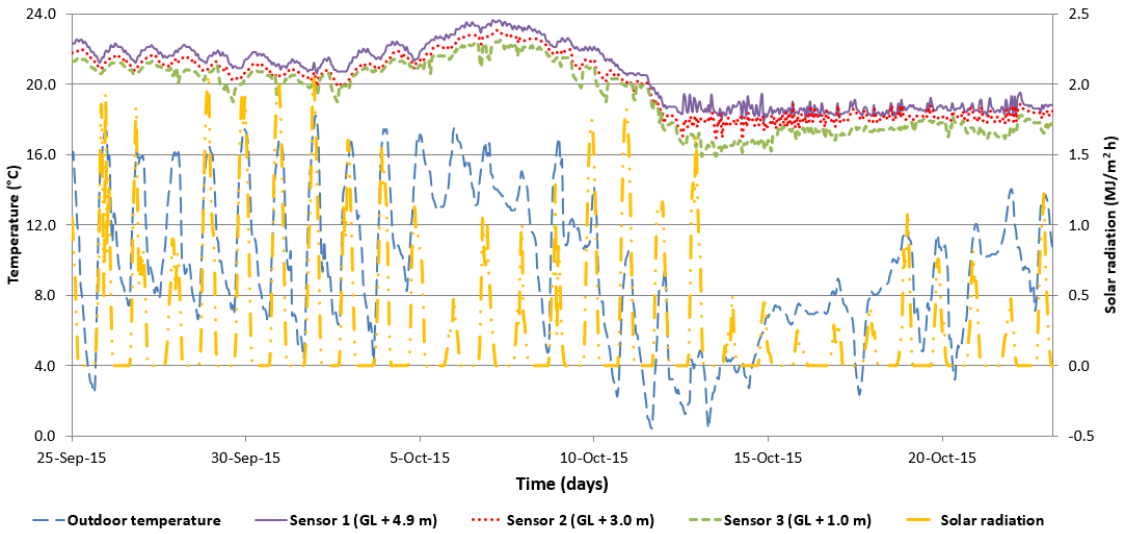

Fig. 6. Measured data at the case object, solar radiation and the outdoor air temperature [39]

the production hall. Using the on-site air temperature measurements of the centrally located sensor (2nd) as a means of calibration, the estimated thermal load and ventilation rate have been adjusted. A comparable method was applied by Jo et al. [37] who used measurement data to determine the thickness of insulation material.

Data from the indoor air temperature sensors and from a nearby KNMI weather station are shown in Fig. 6. The figure shows that the indoor temperature increased with height. During the measurement period, the average outdoor air temperature was 9.6 °C, while the temperature difference between Sensor 1 and Sensor 3 ranged from 0.5 °C to 2.9 °C. After October 13th, the external temperature drops while the internal temperature fluctuates more rapidly, but, as an effect of the installed heating system, hoovers around a reasonably constant average temperature. In the first part of the period, when the heating system was not in use, the temperature in the hall was considerably higher than the outside temperature. This increased temperature can be explained by heat gains from the installed lighting and from the adjacent production hall which generates considerable heat from the installed production equipment.

The heating is implemented in the model by using a continuous heating set point of 17.5 °C based on the measurements taken in the storage hall. Goods stored in the storage hall restrain the internal temperature fluctuations and are modeled as an internal mass based on an estimate by the user of the storage hall of the average contents.

The result of this calibration process is evaluated in terms of the Normalized Mean Bias Error (NMBE), Coefficient of Variation of Root Mean Square Error (CVRMSE) and Correlation Coefficient (R^2) [40], which are three statistical indicators suggested in the ASHRAE Guideline 14-2002 [41]. This resulted in an NMBE of −0.05%, an RMSE of 3.62% and an R^2 of 0.91, all within the acceptable ASHRAE guideline range. In the following sections for each of the five holistic flat roof systems, a description is provided on how it is implemented in the basic model.

3.4.1. Cool roof model

The cool roof concept is implemented in this study as a white-painted roof. This approach is much cheaper than replacing the top layer of the roof albeit not so long-lasting. The albedo of the selected paint (α_c) is 0.7; a value that was also used by Virk et al. [42]. Kolokotroni et al. [12] found in their study an optimum albedo value between 0.6 and 0.7 for their case study on an office building in a comparable climate (London) and a comparable roof structure as in our case study.

The cool roof is simulated based on Eq. (1). The main difference is due to the change in albedo (α_c), which is simulated by decreasing the absorbance of the top layer of the conventional roof.

3.4.2. Green roof model

The green roof modeled in this study is a sedum roof since sedum species are commonly used as they are "really resistant plants which require low maintenance effort thanks to their characteristics of drought resistance and low growing rate" [1]. The green roof is modeled by adding layers to the existing roof. The EcoRoof model uses Eqs. (2) and (3) [23] to calculate the energy balances. The required parameters for the EcoRoof model are extracted from other studies [43,44].

3.4.3. PV panels model

In this study, PV panels are horizontally 'added' above the existing roof, with a ventilated 200 mm gap between the panels and the roof. In the model, the thermal resistance of the PV panels is set at 0.04 m^2K/W and the albedo of the top surface at 0.1 based on manufacturers' specifications and data obtained from Davis et al. [45] and Wang et al. [26].

The PV panels are simulated using Eqs. (4) and (5). They are included as a shading layer above the storage hall using the estimated thermal properties of the PV panels.

3.4.4. Double roof model

In this study, a non-ventilated double roof design is implemented in the form of a non-ventilated cavity with an insulated additional roof-mounted some distance above the existing roof. We added a roof where the emissivity and the albedo values are the same as the existing conventional roof. In this way, we are able to compare the results of adding a second roof and creating a cool roof. The other thermal and physical characteristics of the double roof were set to the values of the Roofclix panels. This then enables us to compare the thermal impact of creating a cool roof, a double roof and installing the Roofclix system.

The double roof is simulated using Eq. (6). In modeling terms, two layers are added on top of the conventional roof: firstly a non-ventilated cavity (25 mm) and then an additional roof layer. For the cavity, a fixed thermal resistance of 0.19 m^2K/W is used as prescribed in ISO 6946 for downward heat flow.

3.4.5. Roofclix model

In January 2010, measurements (conducted by a third party and be available on request) were taken on a building that was partly covered with Roofclix panels. Thermocouples were installed to measure the surface temperatures of the unmodified roof, the roof under the Roofclix panels and the top of the Roofclix panels. The results from 8 January 2010 are shown in Fig. 7 along with the outdoor air temperature using data from the local weather station in the Netherlands at Schiphol Airport [39]. The Roofclix system was initially simulated as prescribed in ISO 6946 using Eq. (7) from Section 3.5. In keeping with ISO 6946, this effectively amounted to adding an additional layer to the conventional roof with a thermal resistance of only

0.06 m^{2}K/W. Using -derived from Fourier's law- Eq. (8) below, the simulation results for the outside surface temperature of the conventional roof are shown in Fig. 8 along with estimates of the surface temperature of the conventional roof, under and without Roofclix.

$$T_r = T_o + \frac{(T_o - T_i)xR_{rx}}{R_r + R_{rx}} \quad (8)$$

Fig. 8 also includes the measured roof surface temperature under the Roofclix panels, and this is consistently higher than the simulated value with an assumed R_{rx} = 0.06 m^{2}K/W. A possible explanation for this consistent difference is that the impact of the Roofclix system is underestimated by ISO 6946. To investigate further, a thermal resistance value for the Roofclix system was determined from the measurements, thereby incorporating the effects of both conductive and convective heat transfer. In effect, we are determining the thermal resistance that, when included in the simulation, produces surface temperatures close to those measured.

Fig. 8 includes the estimated surface temperature under the panels with an assumed thermal resistance of 0.80 m^{2}K/W for the Roofclix system.

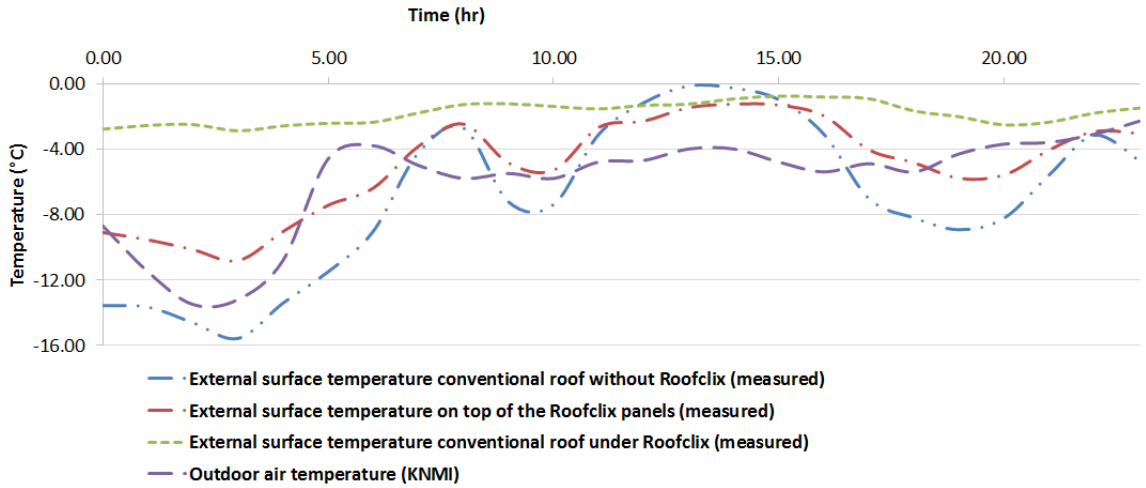

Fig. 7. Measurements with the Roofclix system on 8 January 2010

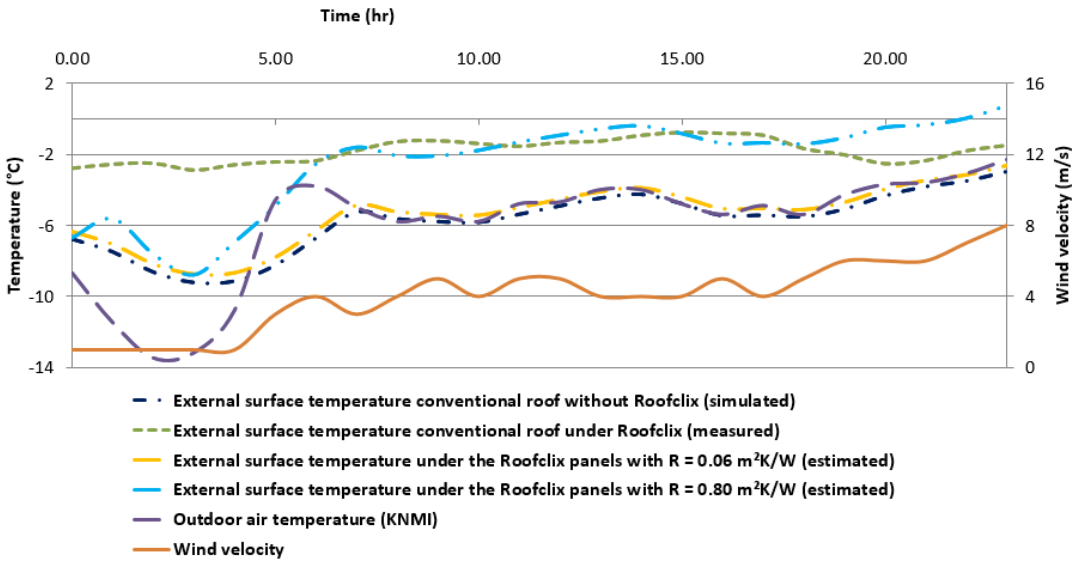

Fig. 8. Simulation and estimation with the Roofclix model

The simulated external surface temperature is reasonably close to the measured value during the main part of the day but in the early hours of the morning, when the outside temperature dropped rapidly and then recovered, the simulated temperatures show a matching, albeit less extreme, pattern whereas the measured surface temperature remained reasonably steady under the Roofclix panels. A possible explanation is that the cavity is not as well ventilated as the simulation assumes and acts more as a closed space below the insulated panels. It would seem that the simplifications used by ISO 6946 fail to model adequately the characteristics of the Roofclix system.

A decreased wind speed decreases the thermal heat flux through a roof [46]. The influence of a decreased wind speed on the thermal resistance of the Roofclix system is calculated using empirical formulae from Eqs. (9)-(11) [13]. This resulted in a thermal resistance for the Roofclix system of 0.77 m^2K/W, a value remarkably close to the earlier estimated value of 0.8 m^2K/W.

$$\mathrm{Re} = \frac{V\,x\,l}{\upsilon} \tag{9}$$

$$Nu = \mathrm{Pr}^{1/3}\; x\left(0.037x\,\mathrm{Re}^{0.8} - 871\right) \tag{10}$$

$$h = \frac{k\;x\;Nu}{l} \tag{11}$$

4. Results and discussion

The desirable internal air temperature in a room depends on many variables, such as the season, the activity level and the thickness of the clothes that people are wearing [47,48]. Here, the Fanger model is widely used to determine the Predicted Mean Vote (PMV), which is a value that estimates the perceived acceptability of the thermal climate in a room [1,17]. Generally, a PMV between -0.5 and 0.5 is considered acceptable in that, within this range, less than 10% of the occupants will be dissatisfied with the conditions [47]. Based on the activities (metabolism = 1.7), relative humidity (RH = 50%) and clothing (clo-value = 0.7) requirements for its users, the Fanger model indicates the acceptable temperature ranges for the storage hall to be 15 − 21.5 °C in winter and 18 – 23 °C in summer [49]. Our simulations show that, in the summer months, the maximum "acceptable" temperature of 23 °C is exceeded on occasions. In order to compare the performance of the various roof structures, we calculate the maximum internal temperature seen throughout the year and the number of times the 23 °C "limit" is exceeded. In this way, we are able to compare the different roof designs in terms of delivering acceptable internal conditions.

4.1. High thermal resistance scenario

The calculated internal air temperature for the conventional roof design with a high thermal resistance is shown in Fig. 9. The internal air temperature is reasonably constant during the winter months at close to the heating set point of 17.5 °C. During the summer months, the internal temperature is driven by the external conditions and peaks at 25.3 °C. However, the external surface temperature of the roof sees a much greater temperature range: from -20.5 °C on 13 February to 70.9 °C on 3 August. The minimum outdoor air temperature was -14.2 °C on 13 February and the maximum 32.8 °C on 4 August. Based on the Fanger model, the maximum acceptable indoor temperature is 23°C, and this was exceeded during 862 hours and by a maximum of 2.3 °C. The corresponding results for the indoor climate with the holistic flat roof systems are shown in Table 2.

4.2. Low thermal resistance scenario

The comparable internal air temperatures for the conventional roof in the low thermal resistance scenario are shown in Fig. 9. The internal air temperature ranges between 17.5 °C and 29.3 °C so, as one might anticipate, reducing the roof insulation results in outside conditions having more influence on internal temperatures. The maximum internal acceptable temperature is now exceeded for 2,155 hours (virtually a quarter of the year) and by as much as 6.3 °C.

The corresponding results for the indoor climate with the various holistic flat roof systems in the low thermal resistance scenario are shown in Table 2.

Table 2. Indoor climate for the holistic flat roof systems

	Cool roof	Green roof	PV panels	Double roof	Roofclix
High thermal resistance scenario					
Number of overheating hours (862)	166	313	139	581	131
Reduction of overheating hours (-)	81%	64%	84%	33%	85%
Maximum internal air temperature (°C)	24.2	24.2	23.8	24.7	23.8
Maximum temperature exceeding (°C)	1.2	1.2	0.8	1.7	0.8
Low thermal resistance scenario					
Number of overheating hours (2,155)	317	722	113	1,366	107
Reduction of overheating hours (-)	85%	66%	95%	37%	95%
Maximum internal air temperature (°C)	25.7	24.9	24.4	26.2	23.9
Maximum temperature exceeding (°C)	2.7	1.9	1.4	3.2	0.9

4.3. Comparison of holistic flat roof systems

The internal air temperature of the storage hall during summer is shown in Fig. 10 for the conventional, high thermal resistance roof, and with each of the holistic flat roof systems applied.

This plot, covering the warmest day of the year, shows that all the holistic flat roof systems decrease the internal air temperature in summer. The number of overheating hours is decreased dramatically by the cool roof (by 81%), the PV panels (by 84%) and the Roofclix system (by 85%) to within the generally accepted number of overheating hours that are tolerated when designing HVAC systems [49]. The maximum overheating is just 0.8 °C for both the PV panels and the Roofclix system. The cool roof simulation indicates a maximum exceedance of 1.2 °C, which is perhaps larger than one might expect given its similar reduction in the number of overheating hours. However, this shows that the effects on the internal air temperature are smaller in case of reflected solar radiation by a cool roof than blocking solar radiation by a cavity under beneath PV panels or Roofclix.

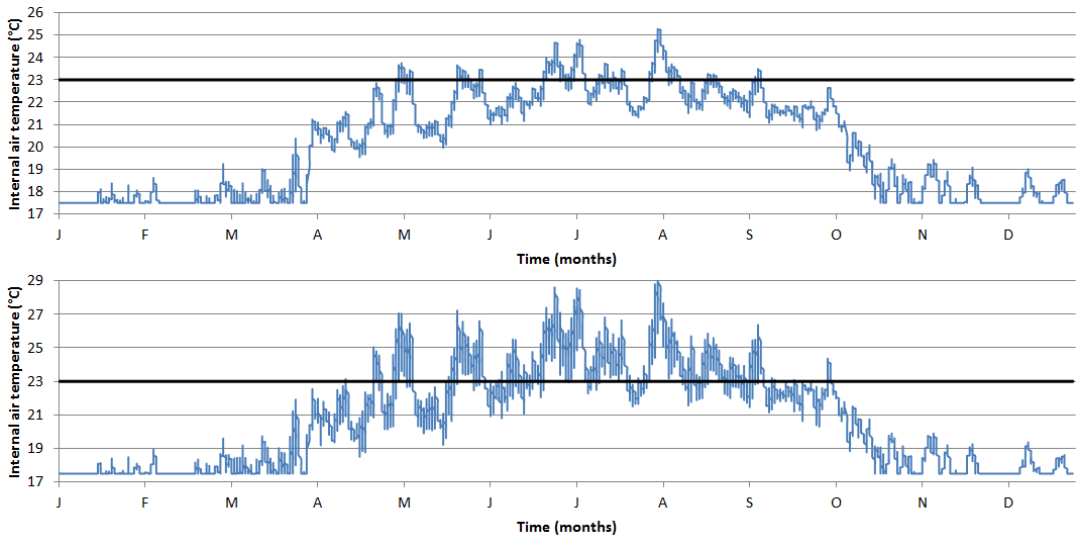

Fig. 9. Simulated internal air temperatures for a conventional high thermal resistance roof (above) and a conventional low thermal resistance roof (below)

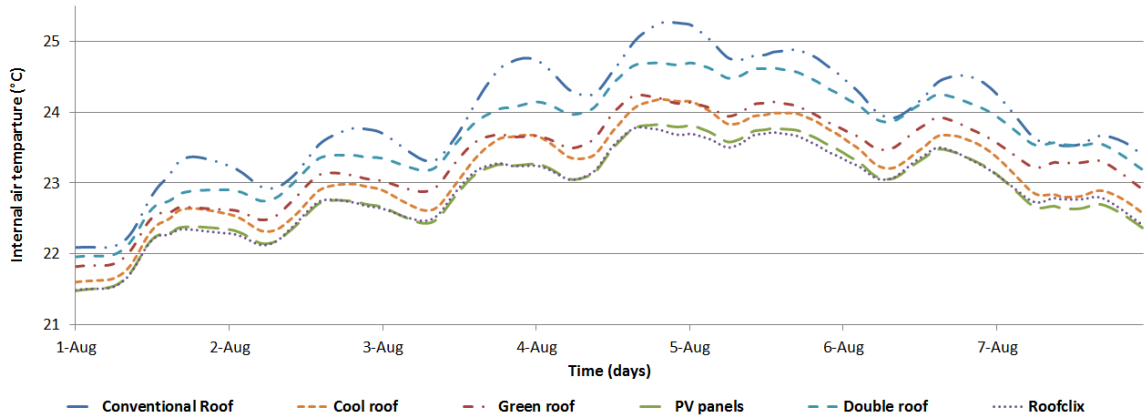

Fig. 10. Simulated internal air temperatures with the holistic flat roof systems.

4.4. Comparison between Roofclix and a combination of cool roof and double roof

For this comparison, the albedo and emissivity values of the cool roof are set to the values of the Roofclix system to be able to compare the results of the Roofclix system, which is a double-skin roof, with a cool roof forming a second roof above the existing roof. Fig. 11 shows that the effect on the internal temperature of a cool double roof has a similar pattern to that of the Roofclix system, but that the temperature decrease is constantly larger than for the Roofclix system. This shows that the combined effect of the high albedo and the increased thermal resistance on the internal temperature is smaller than the individual effects. This can be explained by Fourier's law, that heat transfer is directly proportional to the temperature difference between the inner and outer surface temperatures. A high albedo top layer decreases the external surface temperature, which then decreases the impact of additional insulation. This also shows that simply summing the effects of individual heat transfer methods can lead to incorrect estimates of the impact of holistic flat roof systems.

4.5. Comparison of thermal scenarios

Decreasing the R-value of the thermal shell of the building leads to the solar heat gain by the roof having a larger influence on indoor temperatures. Compared with the more typical roof, the number of overheating hours is more than doubled from 862 to 2,155 and the maximum internal air temperature increases by 4.1 °C. However, the number of overheating hours is lower in the low thermal resistance scenario than in the high thermal resistance scenario for the Roofclix system (18% lower) and when the roof is clad in PV panels (19% lower). An explanation for this could be that the decreased R-value enables more heat to escape from the hall at night [50]. Furthermore, increasing the R-value of the roof from 1.1 m^2K/W for the low thermal resistance scenario to 1.9 m^2K/W for the double roof situation leads to a decrease in the maximum value of the PMV by 0.6, namely from 1.7 to 1.1 [51]. An increase in the thermal resistance of the roof from 3.5 m^2K/W for the high thermal resistance scenario to 4.3 m^2K/W for the double roof situation, decreases the maximum value of the PMV by only 0.1, namely from 0.9 to 0.8. Fig. 12 shows the influence of the R-value of the roof on the internal temperature.

5. Conclusion

The objective of this study has been to analyze the full potential impact of holistic flat roof systems by considering not just conduction, but also convection and radiation in an integrated manner. Our study makes some important scientific contributions. First, the used methodology to assess the impact of holistic flat roof systems provides an

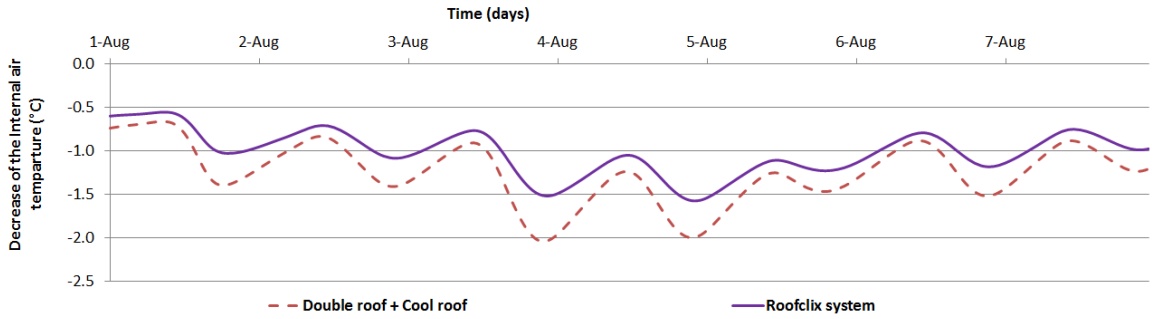

Fig. 11. Simulated decrease in internal air temperatures by applying the Roofclix system or a cool double roof

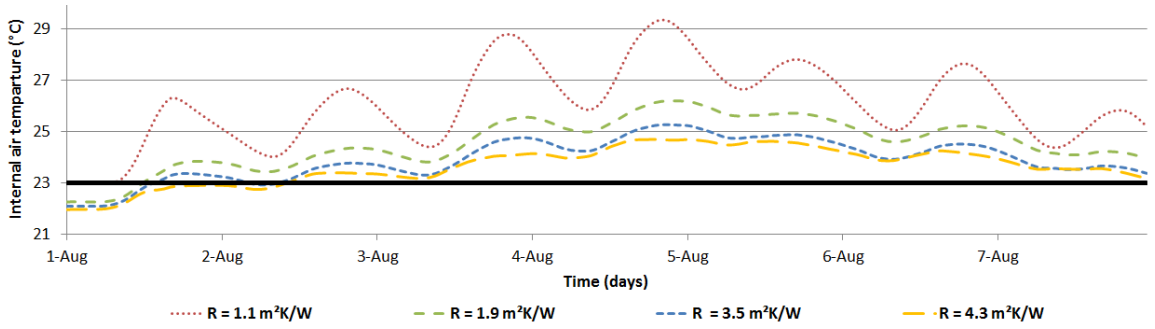

Fig. 12 Simulated influence of the R-value of the roof on internal air temperature.

alternative that includes all three heat transfer methods. This methodology can be applied to other holistic flat roof systems, such as those containing phase change materials [48,52] or a photovoltaic-green roof [53]. Second, it is demonstrated that increasing the thermal resistance of a roof is not only less effective if the roof is already well insulated but that it can also lead to adverse effects.

All the studied holistic flat roof systems can improve the indoor climate in non-cooled buildings which otherwise suffer from overheating in summer. The most effective retrofit systems for decreasing the number of excessively hot hours in a building with a conventional flat roof are the Roofclix system, the cool roof and covering the roof with PV panels, all of which significantly decrease the heat gain by solar radiation. These systems decrease the number of excessively hot hours by 81-85%. These flat roof systems could be an alternative to installing mechanical cooling systems to avoid exceeding the maximum allowable number of overheating hours. In a building with a roof with a low thermal resistance, installing such holistic flat roof systems can decrease the overheated hours by over 90%.

The thermal resistance of an existing roof has a major influence on the effectiveness of adding a holistic flat roof system. For roofs with limited roof insulation, holistic systems that increase the thermal resistance are effective in improving the indoor climate. However, this study shows that increasing the thermal resistance of an existing roof with an R-value greater than 3.5 m^2K/W has little effect on the acceptability of the indoor climate since the improvement according to our simulations in PMV will be less than 0.1. Furthermore, this study shows that, in some situations, increasing the thermal resistance of the roof can lead to an increased number of overheating hours. Therefore, the desirability of changing the thermal resistance of a roof should be carefully determined.

We have shown that to assess the full potential impact of holistic flat roof systems not just conduction, but also convection and radiation,

should be considered. Further, simply combining the thermal impacts of the individual heat transfer methods can lead to misleading conclusions. Therefore, an integrated approach that takes into account the conduction, convection, and radiation of heat, as described in this paper, should be used in assessing holistic flat roof systems.

The findings in this study are relevant for decision-makers who have to assess whether a holistic flat roof system is desirable. Loonen et al. [54] state that decisions in early stages of a building's design have the greatest impact on the final result but are often based on intuition rather than analysis. As such, the methodology used in this study can be useful for building designers in enabling them to compare different holistic flat roof systems in an early design stage. The findings are also relevant for policymakers when addressing Building Codes and Energy Performance Indicators. Often a minimum thermal resistance is stipulated, driving a focus on adding insulation to lower conductivity. However, our findings suggest that solutions that also consider radiation and convection could be highly relevant, especially when it comes to updating existing buildings. In future studies, it would be interesting to study in depth how policy makers could practically increase the use of energy simulation models in regulations.

As with any study, this one has certain limitations. Although two thermal conductivity scenarios and six flat roof systems have been simulated, this study is limited to a single case object. The activities that take place in a building have a large influence on the impact of different holistic flat roof systems and it is quite possible that a different building design would result in different findings. The acceptable temperature range strongly depends on the activities that take place in the building and are also subjected to personal preferences. If work productivity or product quality is increased by improving the indoor climate, this can have significant financial benefits. The thermal characteristics of the rest of a building also have a major influence on the effectiveness of a holistic flat roof system. In this study, the effects of changing the albedo, heat capacity and thermal resistance of the roof were simulated, but there are also other parameters, such as the window-to-wall ratio and the specific heat capacity of the construction elements, that influence the impact of a holistic flat roof system. The shading layers as they are applied in EnergyPlus do not participate in the heat transfer calculations and the longwave radiation between the solar panels and the roof is therefore not included in the calculations. Although limited in size [55], this could have influence on the indoor climate. Incorporating this effect in EnergyPlus would be a valuable follow-up study.

The simulations were performed using weather data for a moderate, northern European, climate. There is also a need to study the effect of holistic flat roof systems on the indoor climate of buildings in other climate zones. In warmer climates, the dominant situation is a downward heat flow with internal heat gain. The described impact of systems that decrease the heat gained through solar radiation will be increased when there are longer periods of overheating. Even in colder climates, holistic flat roof systems might improve the indoor climate since long summer days combined with a thick insulation package can otherwise lead to an accumulation of heat in buildings.

Acknowledgments

The authors would like to express their gratitude to Tebodin for facilitating this research. In particular, we would like to thank Hans Scharpfenecker and Johan van de Wetering for their support and advice.

References

[1] Pisello A. L., Piselli C., Cotana F. Thermal-physics and energy performance of an innovative green roof system: The Cool-Green Roof, Sol. Energy. 116 (2015) 337–356. doi:10.1016/j.solener.2015.03.049.

[2] Sproul J., Wan M. P., Mandel B. H., Rosenfeld A. H. Economic comparison of white, green, and black flat roofs in the United States, Energy Build. 71 (2014) 20–27. doi:10.1016/j.enbuild.2013.11.058.

[3] Dvorak B. Conserving energy with bio-diverse building skins : A review of literature, in: Conf.

Proc. 10th Energy Forum, Bern, 2015: pp. 617–626.

[4] Suehrcke H., Peterson E. L., Selby N. Effect of roof solar reflectance on the building heat gain in a hot climate, Energy Build. 40 (2008) 2224–2235. doi:10.1016/j.enbuild.2008.06.015.

[5] Broks K., van Luijtelaar H. Groene daken nader beschouwd, STOWA and Stichting RIONED, Wageningen, 2015. http://stowa.nl/upload/publicatie2014/Groene Daken voor Presentatie lr.pdf.

[6] Akbari H., Pomerantz M., Taha H. Cool surfaces and shade trees to reduce energy use and improve air quality in urban areas, Sol. Energy. 70 (2001) 295–310. doi:10.1016/S0038-092X(00)00089-X.

[7] Bevilacqua P., Mazzeo D., Arcuri N. Thermal inertia assessment of an experimental extensive green roof in summer conditions, Build. Environ. 131 (2018) 264–276. doi: 10.1016/j.buildenv.2017.11.033.

[8] Entrop B. Assessing energy techniques and measures in residential buildings: a multidisciplinary perspective. PhD-thesis, University of Twente, Enschede, The Netherlands, 2013.

[9] Mohammadian M., Yakhoubi M. Two dimensional laminar natural convection over vaulted and flat roofs exposed to solar radiation, in: Proc. Fourth Int. Conf. Therm. Eng. Theory Appl., Abu Dhabi, 2009: pp. 1–6. http://www.hedcoint.com/Articles and Books/Two dimensional laminar natural convection.pdf.

[10] Chen C. J. Physics of Solar Energy, John Wiley & Sons, Inc., Hoboken, 2011.

[11] Ismail A., Samad M. H. A., Rahman A. M. A. The Investigation of Green Roof and White Roof Cooling Potential on Single Storey Residential Building in the Malaysian Climate, World Acad. Sci. Eng. Technol. 5 (2011) 129.

[12] Kolokotroni M., Gowreesunker B. L., Giridharan R. Cool roof technology in London: An experimental and modeling study, Energy Build. 67 (2013) 658–667. doi:10.1016/j.enbuild.2011.07.011.

[13] Cengel Y. A., Turner R. H. Fundamentals of Thermal-Fluid Sciences, McGraw-Hill Book Co, Singapore, 2001.

[14] Dabaieh M., Wanas O., Hegazy M. A., E. Johansson, Reducing cooling demands in a hot dry climate: A simulation study for non-insulated passive cool roof thermal performance in residential buildings, Energy Build. 89 (2015) 142–152. doi:10.1016/j.enbuild.2014.12.034.

[15] ASHRAE, ASHRAE Standard 90.1-2007: Energy Standard for Buildings Except Low-Rise Residential Buildings, Atlanta, 2007.

[16] Synnefa A., Santamouris M., Akbari H. Estimating the effect of using cool coatings on energy loads and thermal comfort in residential buildings in various climatic conditions, Energy Build. 39 (2007) 1167–1174. doi:10.1016/j.enbuild.2007.01.004.

[17] Ramamurthy P., Sun T., Rule K., Bou-Zeid E. The joint influence of albedo and insulation on roof performance: An observational study, Energy Build. 93 (2015) 249–258. doi:10.1016/j.enbuild.2015.02.040.

[18] Romeo C., Zinzi M. Impact of a cool roof application on the energy and comfort performance in an existing non-residential building. A Sicilian case study, Energy Build. 67 (2013) 647–657. doi:10.1016/j.enbuild.2011.07.023.

[19] Coma J., Pérez G., Solé C., Castell A., Cabeza L. F. Thermal assessment of extensive green roofs as passive tool for energy savings in buildings, Renew. Energy. 85 (2016) 1106–1115. doi:10.1016/j.renene.2015.07.074.

[20] Niachou A., Papakonstantinou K., Santamouris M., Tsangrassoulis A., Mihalakakou G. Analysis of the green roof thermal properties and investigation of its energy performance, Energy Build. 33 (2001) 719–729. doi:10.1016/S0378-7788(01)00062-7.

[21] Gagliano A., Detommaso M., Nocera F., Evola G. A multi-criteria methodology for comparing the energy and environmental behavior of cool, green and traditional roofs, Build. Environ. 90 (2015) 71–81. doi:10.1016/j.buildenv.2015.02.043.

[22] Frankenstein S., Koenig G. FASST Vegetation Models, U.S. Army Corps of Engineers, Washington D.C., 2004.

[23] Sailor D. J. A green roof model for building energy simulation programs, Energy Build. 40 (2008) 1466–1478. doi:10.1016/j.enbuild.2008.02.001.

[24] Dominguez A., Kleissl J., Luvall J. C., Effects of Solar Photovoltaic Panels on Roof Heat Transfer, Sol. Energy. 85 (2007) 2244–2255. doi:http://dx.doi.org/10.1016/j.solener.2011.06.010.

[25] Kotak Y., Gago E., Mohanty P., Muneer T. Installation of roof-top solar PV modules and their impact on building cooling load, Build. Serv. Eng. Res. Technol. 35 (2014) 613–633.

doi:10.1177/0143624414527098.

[26] Wang Y., Tian W., Ren J., Zhu L., Wang Q. Influence of a building's integrated-photovoltaics on heating and cooling loads, Appl. Energy. 83 (2006) 989–1003. doi:10.1016/j.apenergy.2005.10.002.

[27] Kapsalis V. C., Vardoulakis E., Karamanis D. Simulation of the cooling effect of the roof added photovoltaics, Adv. Build. Energy Res. 8 (2014) 41–54. doi:10.1080/17512549.2014.890534.

[28] Zingre K. T., Wan M. P., Wong S. K., Thian Toh W. B., Leng Lee I. Y. Modeling of cool roof heat transfer in tropical climate, Renew. Energy. 75 (2015) 210–223. doi:10.1016/j.renene.2014.09.045.

[29] Biwole P. H., Woloszyn M., Pompeo C. Heat transfers in a double-skin roof ventilated by natural convection in summer time, Energy Build. 40 (2008) 1487–1497. doi:10.1016/j.enbuild.2008.02.004.

[30] Planet Safe, Roofclix, (2010). http://www.meijerman.nl/documentatie/roofclix.pdf (accessed July 13, 2015).

[31] Boyano A., Hernandez P., Wolf O. Energy demands and potential savings in European office buildings: Case studies based on EnergyPlus simulations, Energy Build. 65 (2013) 19–28. doi:10.1016/j.enbuild.2013.05.039.

[32] KNMI, Weerstatistieken De Bilt, (2015). https://weerstatistieken.nl (accessed October 19, 2015).

[33] CBS, Klimaatgegevens; weerstation De Bilt temperatuur, neerslag en zonneschijn, (2015). http://statline.cbs.nl/StatWeb/publication/?VW=T&DM=SLNL&PA=80182NED (accessed October 19, 2015).

[34] Šúri M., Huld T. A., Dunlop E. D., Ossenbrink H. A. Potential of solar electricity generation in the European Union member states and candidate countries, Sol. Energy. 81 (2007) 1295–1305. doi:10.1016/j.solener.2006.12.007.

[35] Bozonnet E., Doya M., Allard F. Cool roofs impact on building thermal response: A French case study, Energy Build. 43 (2011) 3006–3012. doi:10.1016/j.enbuild.2011.07.017.

[36] Berto R., Stival C. A., Rosato P. Enhancing the environmental performance of industrial settlements: An economic evaluation of extensive green roof competitiveness, Build. Environ. 127 (2018) 58–68. doi: 10.1016/j.buildenv.2017.10.032.

[37] Jo J. H., Carlson J. D., Golden J. S., Bryan H. An integrated empirical and modeling methodology for analyzing solar reflective roof technologies on commercial buildings, Build. Environ. 45 (2010) 453–460. doi:10.1016/j.buildenv.2009.07.001.

[38] EN ISO 6946, Building components and building elements-Thermal resistance and thermal transmittance - Calculation method, (2007).

[39] KNMI, Uurgegevens van het weer in Nederland - Download, (2015). http://projects.knmi.nl/klimatologie/uurgegevens/selectie.cgi (accessed November 19, 2015).

[40] Nguyen A. T., Reiter S. An investigation on thermal performance of a low-cost apartment in hot humid climate of Danang, Energy Build. 47 (2012) 237–246. doi:10.1016/j.enbuild.2011.11.047.

[41] ASHRAE, ASHRAE Guideline 14-2002: Measurement of Energy and Demand Savings, Atlanta, 2002.

[42] Virk G., Jansz A., Mavrogianni A., Mylona A., Stocker J., Davies M. Microclimatic effects of green and cool roofs in London and their impacts on energy use for a typical office building, Energy Build. 88 (2015) 214–228. doi:10.1016/j.enbuild.2014.11.039.

[43] Yaghoobian N., Srebric J. Influence of plant coverage on the total green roof energy balance and building energy consumption, Energy Build. 103 (2015) 1–13. doi:10.1016/j.enbuild.2015.05.052.

[44] Stav Y., Lawson G. Vertical vegetation design decisions and their impact on energy consumption in subtropical cities, WIT Trans. Ecol. Environ. 155 (2011) 489–500. doi:10.2495/SC120411.

[45] Davis M. W., Fanney A. H., Dougherty B. P. Prediction of Building Integrated Photovoltaic Cell Temperatures, Trans. ASME. 123 (2001) 200–210. doi:10.1115/1.1385825.

[46] Theodosiou T. G. Summer period analysis of the performance of a planted roof as a passive cooling technique, Energy Build. 35 (2003) 909–917. doi:10.1016/S0378-7788(03)00023-9.

[47] ISSO, Handboek installatietechniek, Instituut voor Studie en Stimulering van Onderzoek op het Gebied van Gebouwinstallaties, Rotterdam, 2002.

[48] Saffari M., De Gracia A., Ushak S., Cabeza L. F. Economic impact of integrating PCM as passive system in buildings using Fanger comfort model, Energy Build. 112 (2016) 159–172. doi:10.1016/j.enbuild.2015.12.006.

[49] ISSO, Addendum Handboek Installatietechniek, Instituut voor Studie en Stimulering van Onderzoek

op het Gebied van Gebouwinstallaties, Rotterdam, 2012. http://www.isso.nl/fileadmin/user_upload/errata/20120601-addendum-hb-i-2012.pdf.

[50] Simpson J. R., McPherson E. G., The effects of roof albedo modification on cooling loads of scale model residences in Tucson, Energy Build. 25 (1997) 127–137. doi:10.1016/S0378-7788(96)01002-X.

[51] ASHRAE, ASHRAE Standard 55-2013: Thermal Environmental Conditions for Human Occupancy, Atlanta, 2013.

[52] Roman K. K., O'Brien T., Alvey J. B., Woo O. Simulating the effects of cool roof and PCM (phase change materials) based roof to mitigate UHI (urban heat island) in prominent US cities, Energy. 96 (2016) 103–117. doi:10.1016/j.energy.2015.11.082.

[53] Hui S. C. M., Chan S. C. Integration of green roof and solar photovoltaic systems, Jt. Symp. 2011 Integr. Build. Des. New Era Sustain. 2011 (2011) 1–12.

[54] Loonen R. C. G. M., Singaravel S., Trčka M., Cóstola D., Hensen J. L. M. Simulation-based support for product development of innovative building envelope components, Autom. Constr. 45 (2014) 86–95. doi:10.1016/j.autcon.2014.05.008.

[55] Phiraphat S., Prommas R., Puangsombut W. Experimental study of natural convection in PV roof solar collector, International Communications in Heat and Mass Transfer. 89 (2017) 31–38. doi: 10.1016/j.icheatmasstransfer.2017.09.022.

Nomenclature

d	thickness material (m)
F	net heat flux (W/m^2)
h	convection heat transfer coefficient (W/m2K)
H	sensible heat flux (W/m^2)
I	total incoming radiation (W/m^2)
k	thermal conductivity of air (W/mK)
l	characteristic length of the roof (m)
L	latent heat flux (W/m^2)
Nu	Nusselt number (-)
Pr	Prandtl number (-)
R	thermal resistance (m^{2}K/W)
Re	Reynolds number (-)
T	surface temperature (K)
T_o	outside air temperature (K)
T_{sky}	effective sky temperature (K)
V	wind speed (m/s)

Greek letters

α	albedo (-)
ε	emissivity (-)
λ	thermal conductivity (W/mK)
υ	kinematic viscosity (m^2/s)
ρ	density (kg/m3)
σ	Stefan-Boltzmann constant (5.67 x 10^{-8} W/m^{2}K^4)
σ_f	fractional vegetation cover (-)

Subscripts

b	back side PV panels
c	cool roof
cav	cavity
f	foliage layer
g	ground layer
i	internal
ir	longwave infrared radiation
PV	photovoltaic panels
r	conventional roof
rx	Roofclix system
s	shortwave solar radiation
dr	double roof
t	top side PV panels